SPECIAL PROJECT PROGRESS REPORT

All the following mandatory information needs to be provided. The length should *reflect the complexity and duration* of the project.

Reporting year	2019
Project Title:	Simulating the green Sahara with EC-Earth 3.2
Computer Project Account:	SPSEZHAN
Principal Investigator(s):	Qiong Zhang
Affiliation:	Department of Physical Geography Stockholm University
Name of ECMWF scientist(s) collaborating to the project (if applicable)	
Start date of the project:	2019-01-01
Expected end date:	2021-12-31

Computer resources allocated/used for the current year and the previous one

(if applicable)

Please answer for all project resources

		Previous year		Current year	
		Allocated	Used	Allocated	Used
High Performance Computing Facility	(units)	15.000.000	16.447.687	20.000.000	9.930.312
Data storage capacity	(Gbytes)	5000	5000	5000	2000

Summary of project objectives (10 lines max)

We aim to run transient simulations to investigate the termination of Green Sahara. The planned transient simulation will be about 3500 years long from 8000 BP (8ka) to 4500 BP (4.5ka). This simulation will provide a comprehensive understanding of the vegetation feedbacks in the transition phases together with the possibility of having multiple equilibria in Northern Africa. Besides the transient simulations, different sensitivity simulations will be also performed to understand the climate response and feedbacks, such as offline dynamical vegetation model simulations to determine how much precipitation would be needed to initiate a green Sahara. We also test the impact of the aerosol direct and indirect effect through a few sensitivity experiments.

Summary of problems encountered (10 lines max)

All the simulations are going on well and in the production run, no problems encountered this year.

Summary of plans for the continuation of the project (10 lines max)

From 2019 to 2020, we have done several equilibrium experiments with the coupled dynamical vegetation model LPJ-GUESS to EC-Earth under the climate condition pre-industrial (1850), mid-Holocene (6 ka) and last interglacial (127 ka). We also finished the spin-up run for the starting year 8ka BP and have started the transient simulation from 8 ka to 4.5 ka with varied orbital forcing and GHG forcing. We also started a parallel transient simulation from 127 ka to 125 ka, by using the computation resource in NSC (National Supercomputer Centre in Sweden). This will give us insight if a green Sahara can be initiated during the last interglacial period when the climate warmer than the current interglacial.

List of publications/reports from the project with complete references

The publications listed below during project year 2019 have acknowledged the HPC and data support from ECMWF. Some works may have done during the previous years. The results from paper 4-6 are summarized with a few representative illustrations below.

1. Aichner, B., Z. Makhmudov, I. Rajabov, Q. Zhang, F.S.R. Pausata, M. Werner, L. Heinecke, M. Kuessner, S. Feakins, D. Sachse, and S. Mischke, 2019: Hydroclimate in the Pamirs was driven by changes in precipitation-evaporation seasonality since the last glacial period, Geophysical Research Letters. 46, 13,972–13,983. https://doi.org/10.1029/2019GL085202
2. Han Z., S. Tao, Q. Zhang, Q. Wen, and G. Feng, 2019: Thermodynamic and dynamic effects of increased moisture source over the Tropical Indian Ocean in recent decades, Climate Dynamics, 53, 7081-7096, https://doi.org/10.1007/s00382-019-04977-w.
3. Scussolini, P., P. Bakker, C. Guo, C. Stepanel, Q. Zhang, P. Braconnot, J. Cao, M. Guarino, D. Coumou, M. Prange, P.J. Ward, H. Renssen, M. Kageyama, B. Otto- Bliesner, and J.C.J.H. Aerts, 2019: Agreement between reconstructed and modeled boreal precipitation of the Last Interglacial, Science Advances, **5**.
4. Piao, J., W. Chen, L. Wang, F.S.R. Pausata, Q. Zhang, 2019: Northern extension of the East Asian summer monsoon during the mid-Holocene, Global and Planetary Change, https://doi.org/10.1016/j.gloplacha.2019.103046.
5. Sun, W., B. Wang, Q. Zhang, F. S. R. Pausata, D. Chen, G. Lu, M. Yan, L. Ning, and J. Liu, 2019: Northern Hemisphere Land Monsoon Precipitation Increased by the Green Sahara During Middle Holocene, Geophysical Research Letters, doi: 10.1029/2019gl08211.
6. Lu, Z., P.A. Miller, Q. Zhang, D. Wårlind, L. Nieradzik, J. Sjolte, Q. Li and B. Smith, 2019: Vegetation pattern and terrestrial carbon variation in past warm and cold climates. Geophysical Research Letters, 46, 8133–8143. https://doi.org/10.1029/ 2019GL083729

Summary of results

If submitted **during the first project year**, please summarise the results achieved during the period from the project start to June of the current year. A few paragraphs might be sufficient. If submitted **during the second project year**, this summary should be more detailed and cover the period from the project start. The length, at most 8 pages, should reflect the complexity of the project. Alternatively, it could be replaced by a short summary plus an existing scientific report on the project attached to this document. If submitted **during the third project year**, please summarise the results achieved during the period from July of the previous year to June of the current year. A few paragraphs might be sufficient.

Here we summarised the published results that are most relevant to the green Sahara project. The report includes the impact of Greening of Sahara on east Asian monsoon and global land monsoon. The model experiments used in these works are summarised in table 1. Second part is on the sensitivity experiments with dynamical vegetation model LPJ-GUESS model in past cold and warm climate.

Table 1
Description of the Model Experiments and Net Effect of Each Forcing

Simulation	Orbital forcing	GHGs	Saharan vegetation	Dust concentration
PI	1,850 AD	1,850 AD	Desert	PI
PI_{GS}	1,850 AD	1,850 AD	Shrub	PI
MH_{ORB}	6,000 year BP	6,000 year BP	Desert	PI
MH_{GS}	6,000 year BP	6,000 year BP	Shrub	PI
MH_{GSRD}	6,000 year BP	6,000 year BP	Shrub	Reduced

Abbreviation	Net effect of each forcing	Equation
ORB	Effect of orbital/GHGs forcing during the mid-Holocene	MH_{ORB}–PI
GS	Net effect of vegetation change during the mid-Holocene	MH_{GS}–MH_{ORB}
GS_{PI}	Net effect of vegetation change during the preindustrial	PI_{GS}–PI
GSRD	Combined effect of vegetation change and dust reduction during the mid-Holocene	MH_{GSRD}–MH_{ORB}

Northward extension of the East Asian summer monsoon during the mid-Holocene due to the greening of Sahara (Piao et al., 2019)

Summary. This work is based on our sensitivity experiments by changing the vegetation cover and dust emission during mid-Holocene (MH). The results show that considering a vegetated and dust-reduced Sahara in the MH can significantly strengthen the east Asian summer monsoon (EASM) intensity (Fig. 1).and expand its northernmost boundary northward (Fig. 2) compared to the results with orbital forcing alone. The vegetation change over the Sahara is the dominant factor for the variation in the EASM, while the dust reduction plays a smaller role. The vegetated Sahara causes a westward shift of the Walker circulation, accompanied with enhancement of the western Pacific subtropical high (WPSH), which then results in a strengthened EASM. On one hand, the change in the Walker circulation induces decreased rainfall over the western equatorial Pacific, intensifying the WPSH through the Gill-Matsuno response. On the other hand, the shift in the Walker circulation is associated with a stronger local Hadley circulation, reinforcing the WPSH. Finally, our results show that the westward expansion of the WPSH is mainly caused by the local strengthening of the Hadley circulation.

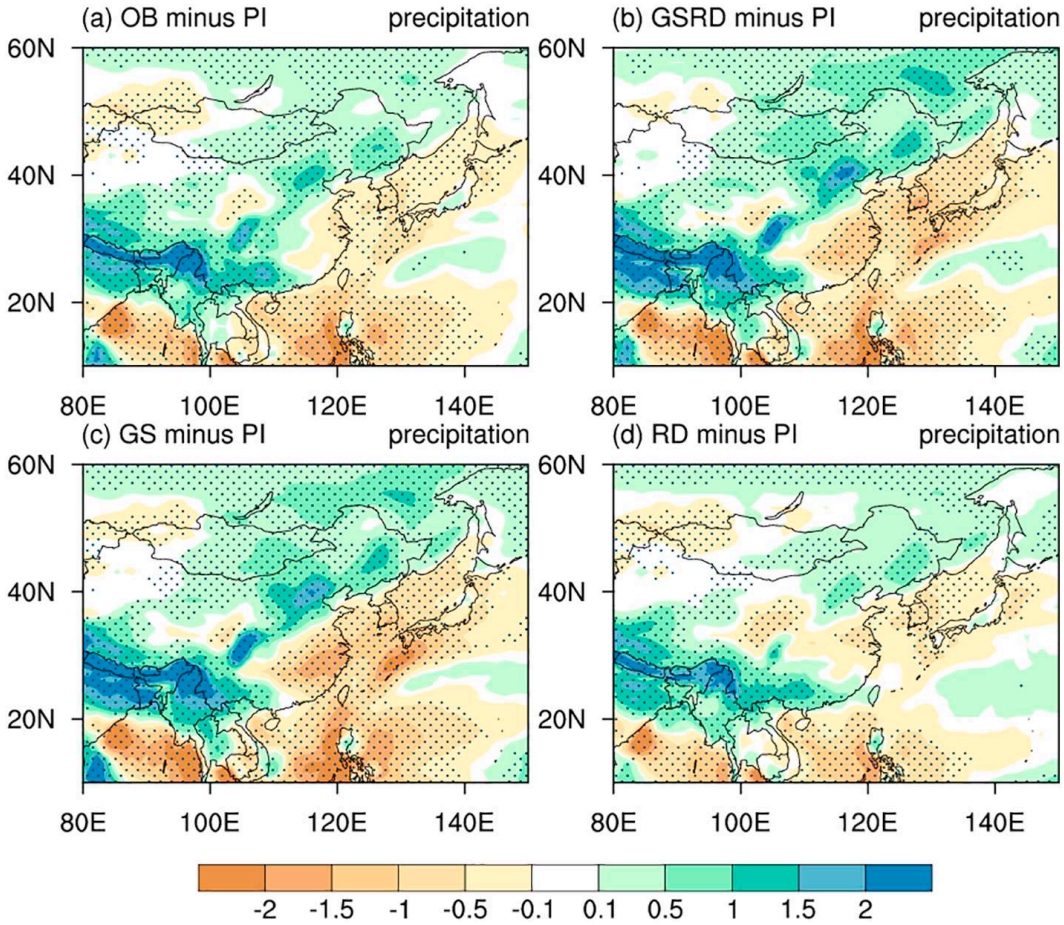

Figure 1. Summer (June to August) mean anomalies in precipitation (shadings, mm/day) between the (a) MHOB, (b) MHGS+RD, (c) MHGS, (d) MHRD and the reference PI experiment. The dotted areas denote the differences significant at the 95% confidence level by the Student t-test.

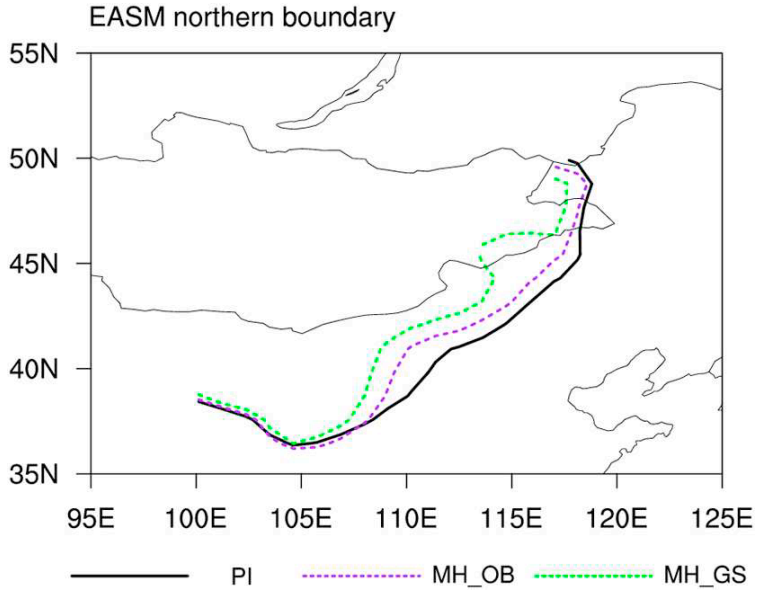

Figure 2. The climatological mean position of the EASM northern boundary in the PI (black solid line), the MHOB (purple dotted line), and the MHGS (green dotted line). (For interpretation of the references to colour in this figure legend, the reader is referred to the web version of this article.)

Northern Hemisphere Land Monsoon PrecipitationIncreased by the Green Sahara During Middle Holocene (Sun et al., 2019)

Summary. Here we show that during the mid-Holocene, most of the Northern Hemisphere land monsoon precipitation (NHLMP) changes revealed by proxy data are reproduced by the Earth System model results when the Saharan vegetation cover and dust reduction are taken into consideration. The simulated NHLMP significantly increases by 33.10% under the effect of the Green Sahara (Fig. 3). The North African monsoon precipitation increases most significantly. Additionally, the Saharan vegetation (dust reduction under vegetated Sahara) alone remotely intensifies the Asian (North American) monsoon precipitation through large-scale atmospheric circulation changes. These findings imply that future variations in land cover and dust emissions may appreciably influence the NHLMP.

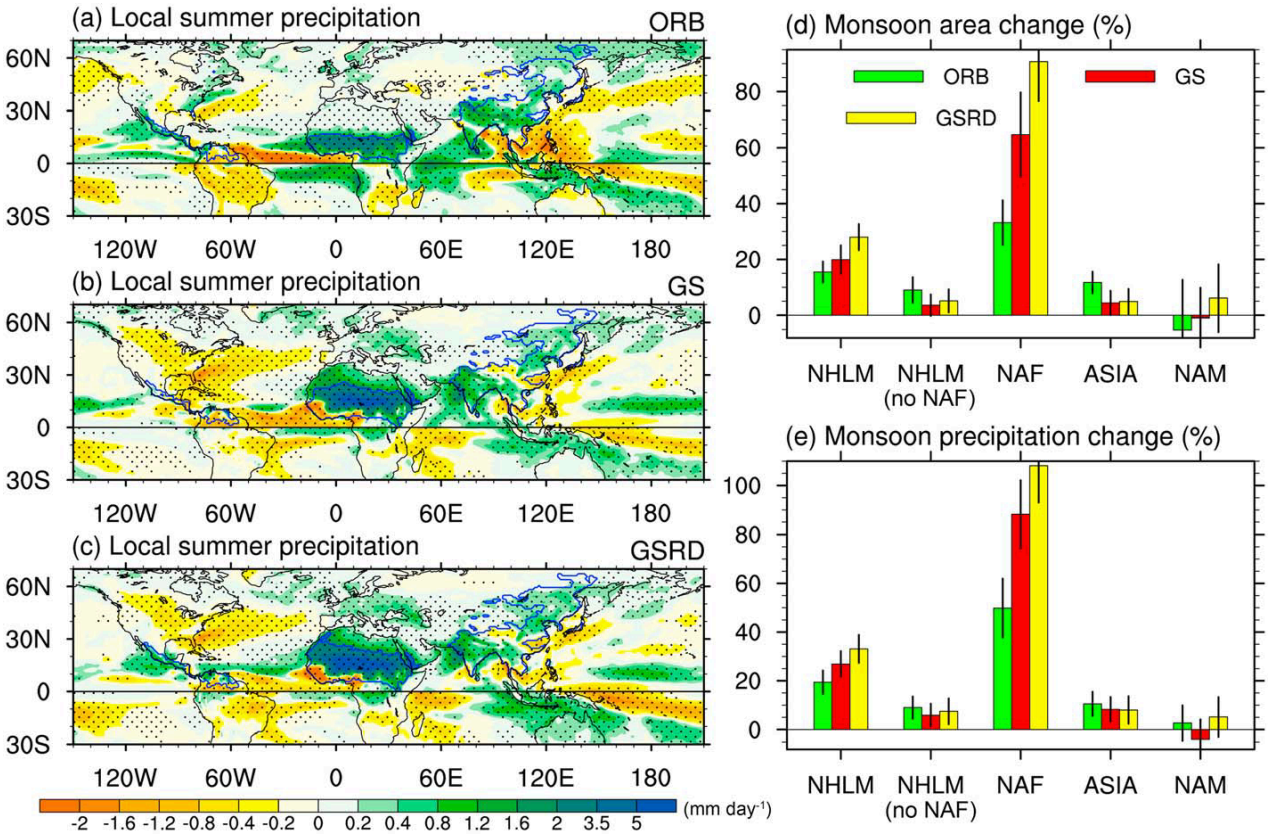

Figure 3. Land monsoon precipitation changes. (a–c) Local summer precipitation anomalies (mm/day) under ORB, GS, and GSRD, respectively. Local summer represents May to September in NH and November to March in SH. Blue lines in a–c highlight the land monsoon areas in the MHORB, MHGS, and MHGSRD experiments, respectively. The dots denote areas in which the changes are significant at the 95% confidence level via a two-tailed Student's t test. (d and e) Change rates (%) in land monsoon area and precipitation, respectively. Monsoon regions include NHLM, North African NAF), Asian (ASIA), and North American (NAM) monsoon. “No NAF” denotes the area that does not include the North African monsoon. Green bars represent the results in ORB, red bars represent the results in GS, and yellow bars denote the results in GSRD. The black vertical lines over the bars show the range of one standard deviation.

Vegetation pattern and terrestrial carbon variation in past warm and cold climates (Lu et al., 2019)

Summary. Using a dynamic vegetation model LPJ-Guess, we simulate vegetation distribution and terrestrial carbon cycling in past cold and warm climates and elucidate the forcing effects of temperature, precipitation, atmospheric CO_2 concentration (pCO_2), and landmass. Results are consistent with proxy reconstructions and reveal that the vegetation extent is mainly determined by temperature anomalies, especially in a cold climate, while precipitation forcing effects on global-scale vegetation patterns are marginal (Fig. 4). The pCO_2 change controls the global carbon balance with the fertilization effect of higher pCO_2 linking to higher vegetation coverage, an enhanced terrestrial carbon sink, and increased terrestrial carbon storage (Fig. 5). Our results indicate carbon transfer from ocean and permafrost/peat to the biosphere and atmosphere and highlight the importance of forest expansion as a driver of terrestrial ecosystem carbon stock from cold to warm climates.

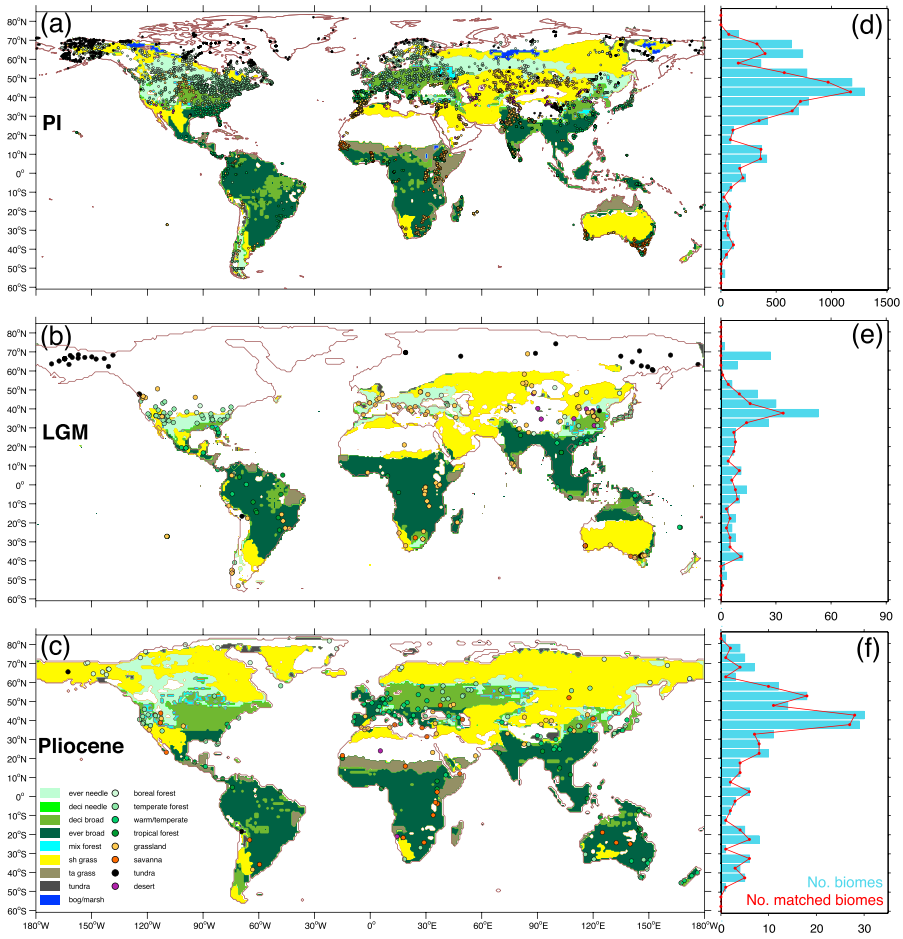

Figure 4. (a–c) Maps of dominant vegetation types for pre-industrial period (PI), Last Glacial Maximum (LGM), and Pliocene simulated by LPJ-GUESS (shading color). Bare soil (white color) is specified where vegetation cover is less than 20%. Circles are reconstructed biomes. (d–f) Distribution of the biome records by latitude (blue histogram) in 5° steps. Red curves show distribution of biome records matched with simulation results.

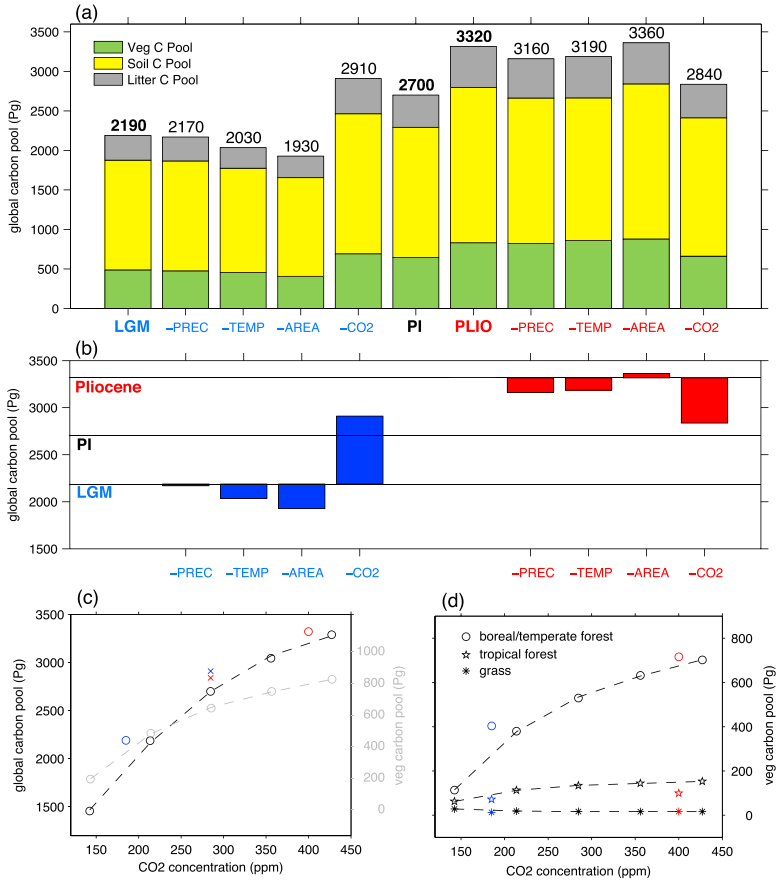

Figure 5. (a) Simulated global terrestrial carbon storage for all simulations (bars, with different colors showing vegetation, soil, and litter carbon pools, respectively). (b) The differences between sensitivity experiments and baseline simulations. (c) The total terrestrial carbon pool and vegetation carbon pool for pCO_2 sensitivity experiments (black and gray circles), Last Glacial Maximum (LGM; blue circle, blue crosses for LGM−CO_2), and Pliocene (red circle, red crosses for Pliocene−CO_2). The dashed lines are the third-degree polynomial fitting lines. (d) Same as (c) but for the individual vegetation carbon pools. PI = pre-industrial period.